Original Article
J Vet Sci 2015, 16(3), 349-356 · http://dx.doi.org/10.4142/jvs.2015.16.3.349

Air assisted lamellar keratectomy for the corneal haze model

Soohyun Kim[1], Young Woo Park[1], Euiri Lee[1], Sang Wan Park[1], Sungwon Park[1], Jong Whi Kim[2], Je Kyung Seong[2], Kangmoon Seo[1,*]

Departments of [1]Veterinary Clinical Science and [2]Veterinary Biomedical Science, Research Institute for Veterinary Science, College of Veterinary Medicine, Seoul National University, Seoul 151-742, Korea

To standardize the corneal haze model in the resection depth and size for efficient corneal haze development, air assisted lamellar keratectomy was performed. The *ex vivo* porcine corneas were categorized into four groups depending on the trephined depth: 250 μm (G1), 375 μm (G2), 500 μm (G3) and 750 μm (G4). The stroma was equally ablated at the five measurement sites in all groups. Significant differences were observed between the trephined corneal depths for resection and ablated corneal thickness in G1 ($p < 0.001$). No significant differences were observed between the trephined corneal depth for resection and the ablated corneal thickness in G2, G3, and G4. The resection percentage was similar in all groups after microscopic imaging of corneal sections. Air assisted lamellar keratectomy (AK) and conventional keratectomy (CK) method were applied to six beagles, after which development of corneal haze was evaluated weekly until postoperative day 28. The occurrence of corneal haze in the AK group was significantly higher than that in the CK group beginning 14 days after surgery. Alpha-smooth muscle actin expression was significantly higher in the AK group ($p < 0.001$) than the CK group. Air assisted lamellar keratectomy was used to achieve the desired corneal thickness after resection and produce sufficient corneal haze.

Keywords: ablated corneal depth, air assisted lamellar keratectomy, canine eye, corneal haze, porcine eye

Introduction

Corneal transparency, which is one of the most important factors influencing vision, is a functional translation of the detailed ultrastructure of the stroma that is primarily attributed to the narrow, uniform diameter of collagen fibrils [13]. Corneal haze is associated with disruption of the collagen fiber array [16] and proliferation of newly formed myofibroblasts during the fibrotic response [6]. The development of corneal haze resulting from refractory corneal diseases and photorefractive keratectomy (PRK) has been reported [19]. Although fibrotic response is an essential component of the normal corneal healing process [9], significant corneal opacity can be induced during this process and mediate a decline in visual acuity. Therefore, a crucial aspect of corneal wound healing is minimizing corneal haze.

Several experimental models have been introduced in the effort to develop treatments to prevent or reduce corneal haze, including mechanical debridement, chemical burning, and PRK [3,20,23]. Corneal wound healing is a complex process controlled by various factors [21], and the size and depth of experimental corneal defects are important factors that must be considered for objective experimental modeling. The desired resection depth is not easily attained using experimental methods that include mechanical debridement and chemical burns. Conversely, PRK is better able to achieve the desired ablation thickness, but requires specialized expensive laser equipment. Thus, there is a need for a standardized and easily applied method.

Anwar and Teichmann introduced the big-bubble technique (BBT) to expose Descemet's membrane by injecting air into the deep stroma [1]. In this method, the stromal structure is deformed to become loose, and a large bubble is made between the deep stroma and the Descemet's membrane by injecting air. A very small stromal layer resided after applying this method [11]. When this technique was applied, the injected air blanched the stroma, resulting in loss of transparency. In this study, the air injection method was applied to the partial stromal layer with slight modification for blanching to acquire the desired depth.

Received 26 Nov. 2014, Revised 3 Feb. 2015, Accepted 7 Mar. 2015
*Corresponding author: Tel: +82-2-880-1258; Fax: +82-2-883-8651; E-mail: kmseo@snu.ac.kr
pISSN 1229-845X
eISSN 1976-555X

This method permitted visualization of the superficial stroma and the loosely deformed stromal structure.

The purpose of this study was to establish a standardized corneal haze model for wound size and depth by using air assisted lamellar keratectomy, which is a modification of the big bubble technique. Additionally, the occurrence of corneal haze resulting from the air assisted lamellar keratectomy was evaluated by comparing it with the occurrence of corneal haze resulting from the conventional method.

Materials and Methods

Experimental design

Fifty porcine and 12 canine eyes were used in this study. Ten porcine eyes were included in each group according to the trephined corneal depth for resection of 250 (G1), 375 (G2), 500 (G3), and 750 μm (G4). Ten eyes were used to make histopathological sections of normal corneas (n = 5) and air-injected corneas (n = 5).

Six female beagles were used. One eye of each dog was selected at random for air assisted lamellar keratectomy (AK group; three right and three left eyes, n = 6), while the contralateral eye received a conventional superficial lamellar keratectomy (CK group; three right and three left eyes, n = 6). Basal corneal haze and corneal haze was evaluated *in vivo* at 7, 14, 21, and 28 days after surgery. The dogs were sacrificed 4 weeks postoperatively for periodic acid Schiff (PAS) and immunofluorescent (anti α-SMA antibody) staining to study the formation of myofibroblasts.

Animals

Fifty porcine eyes obtained from a slaughterhouse and six healthy female beagles were used. Prior to the experiment, all dogs underwent an ophthalmic examination including slit-lamp biomicroscopy (SL-D7; Topcon, Japan), indirect ophthalmoscopy (Vantage plus; Keeler Ophthalmic Instruments, UK), rebound tonometry (Tonovet; Tiolat, Finland), Schirmer's tear test I (Schirmer tear test; Intervet, USA) and fluorescein staining (Fluorescein paper; Haag Streit Diagnostics, Switzerland), and dogs with ocular or systemic diseases were excluded. The animal use and experimental protocols were approved by the Institutional Animal Care and Use committee (SNU-121108-4 and 121123-10; Seoul National University, Korea).

Ex vivo experiments on porcine eyes (air assisted lamellar keratectomy)

Porcine eyes were placed on a specially designed frame (panel A in Fig. 1). The intraocular pressure (IOP) was 10 to 20 mmHg as measured by an applanation tonometer (TonoPen XL; Mentor, USA). The center of the cornea was trephined to 250 (G1), 375 (G2), 500 (G3), and 750 μm (G4) using an 8 mm diameter trephine (Barron radial vacuum trephine; Katena Products, USA). The surgical field was kept dry after trephination to minimize stromal edema. A 30 gauge needle was attached to a 4 mL air-filled syringe. The needle was bent 5 mm from its tip so that the terminal segment angled upwards at approximately 60^{o}, while the bevel faced up. The tip was introduced parallel to the corneal surface into the central stroma at the base of the trephination groove (panels B-F in Fig. 1). The plunger of the air-filled syringe was pressed until intrastromal blanching was observed. The fuzzy region of the white opaque cornea was removed using a corneal dissector and blunt-tipped corneal scissors.

Corneal thickness was measured at five places (the central, superior, inferior, nasal, and temporal surface) within the

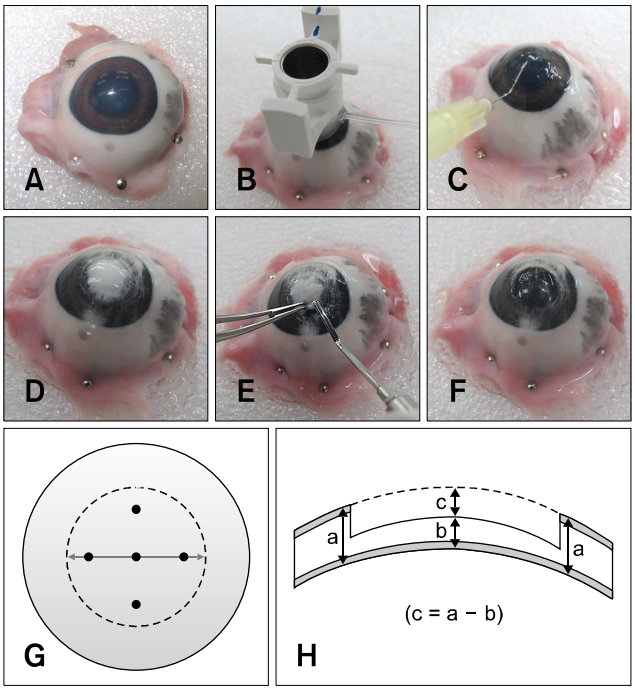

Fig. 1. Air assisted lamellar keratectomy. (A) The enucleated porcine eye was placed on a specially designed frame. (B) The center of the cornea was trephined using a vacuum trephine. (C) Four mL of air was injected at the base of the trephination gutter into the corneal stroma using a 30-gauge needle attached to a syringe. (D) Intrastromal blanching was observed. (E) The blanched cornea was removed using a corneal dissector and blunt-tipped corneal scissors. (F) Appearance after keratectomy using air assisted lamellar keratectomy. (G) Schematic diagrams for measuring corneal thickness. The dotted line indicates the ablated corneal area and the arrows show an 8 mm diameter. The measurement sites of corneal thickness by ultrasonic pachymeter are marked by black dots. (H) Diagram of the corneal cross section. The thickness of the ablated area (b) was subtracted from the normal corneal thickness (a) to calculate the ablated corneal thickness (c).

central 8 mm diameter area of the cornea using an ultrasonic pachymeter (Pachmete DGH 55; DGH Technology, USA) before and after applying the air assisted lamellar keratectomy (panel G in Fig. 1). The pachymetry values are expressed as the average ± standard deviation (SD) of 25 successive readings. If the SD of a measurement was > 10 μm, the value was discarded. Ablated corneal depth was calculated using the corneal thickness pre- and post-operation, and the calculated thickness and trephined depth were compared.

In vivo experiments on canine eyes (anesthesia and surgical procedures)

Each dog was positioned in dorsal recumbency while under general anesthesia. The head was stabilized with a vacuum pillow, and the ocular surface was disinfected with 0.5% povidone iodine solution. Upper and lower eyelids were braced using an eyelid speculum. Keratectomy was performed in the two groups using either air assisted lamellar keratectomy (AK group) or conventional keratectomy (CK group) after administration of atracurium (0.01 mg/kg, IV, Atra injection; Hana Pharm, Korea) for central positioning of the cornea. The center of the cornea was trephined for 375 μm using an 8 mm diameter trephine in both groups. A conventional superficial keratectomy was performed with a lamellar blade no. 66. Following surgery, one drop of atropine (1%, ISOPTO Atropine; Alcon, Belgium) was applied only once. Additionally, one drop of levofloxacine (0.5%, Cravit; Daiichi Sankyo, Japan) was applied three times daily until day 7 after surgery in all groups.

Clinical grading of corneal haze

The level of haze in the cornea was measured by slit lamp biomicroscopy (SL-D7; Topcon) at 7, 14, 21, and 28 days after surgery and graded as follows [5]: Grade 0, completely clear cornea; Grade 0.5, trace haze seen with careful oblique illumination; Grade 1, mild obscuration of iris details; Grade 2, a more prominent haze not interfering with visibility of fine iris details; Grade 3, moderate obscuration of the iris and lens; Grade 4, complete opacification of the stroma in the area of ablation. Haze grading was performed in a blinded manner by three independent veterinarians.

Quantitative corneal haze grading

The slit images were taken under standardized conditions (1 mm wide, 14 mm long slit beam and a 45° angle from the temporal aspect of the cornea without background illumination to evaluate corneal haze preoperatively) at 7, 14, 21, and 28 days post-surgery. Each photograph was converted to an 8 bit gray-scale image using digital image analysis software (ImageJ ver. 1.46r; National Institutes of Health, USA). The selected area of the corneal section (100 × 3 pixels) was isolated, and an intensity of 0 to 255 was determined by averaging the gray-scale (intensity) indices of individual pixels within the area. Total intensity levels within the selected area were measured.

Histopathological and immunofluorescence analyses

Beagle eyes were enucleated by the conventional trans-scleral method after euthanasia. Porcine and canine corneas were excised from the globe by cutting with a blade and tenotomy scissors 2 to 3 mm from the limbus. Samples were fixed in 10% buffered formalin and embedded in paraffin. Sections were stained with PAS according to the standard procedure. A light microscope (BX51; Olympus, Japan) equipped with a digital camera (DP71; Olympus) was used for photomicrography. The thickness of the non-ablated and ablated corneas on the histopathological section was determined by digital image analysis and the percentage of the ablated corneal thickness was calculated (panel H in Fig. 1).

Immunofluorescent staining for α-smooth muscle actin (SMA), a marker for myofibroblasts, was performed in the canine eyes using mouse monoclonal antibody for α-SMA (Dako, USA) with Alexa Fluor 488 goat anti-mouse IgG secondary antibody (Molecular Probes, USA). The immunohistochemistry slides were mounted with SlowFade Gold antifade reagent with DAPI (Molecular Probes) and imaged using a fluorescence microscope (BX51; Olympus) equipped with a digital camera (DP71; Olympus).

Quantification of α-SMA positive cells

The α-SMA positive cells in six randomly selected, non-overlapping, full-thickness central corneal columns, extending from the anterior stromal surface to the posterior stromal surface, were counted as previously described [14]. Images were evaluated by digital image analysis.

Statistical analysis

All measurements were performed in triplicate, and the results are expressed as the mean ± SD. Statistical analyses were performed using SPSS V20 for Windows (SPSS, USA). A Student's *t*-test was used to test for significance between the two groups. One way analysis of variance (ANOVA) with Bonferroni's post-hoc assessment was employed to test for significance when comparing three or more groups. P values < 0.05 were considered significant.

Results

The mean IOP before trephination was 13.7 ± 0.2 mmHg (range, 11.3–16.0 mmHg) after fitting the eyes on the specially designed frame. No significant differences were observed between the mean IOP of each group based on one-way ANOVA with Bonferroni's post-hoc test ($p = 0.957$). Mean corneal thickness pre- and post-operation and the ablated

cornea for each of the five measurement sites are shown in Table 1. No significant differences were observed among the five measurement sites within each group. The ablated corneal thickness in G1 ($p < 0.001$) was significantly different from the trephined corneal depth (Table 2). No significant differences were detected between ablated corneal thickness and the trephined corneal depth for resection in G2 ($p = 0.214$), G3 ($p = 0.381$) or G4 ($p = 0.439$).

No significant differences were observed between the ablated percentages measured by ultrasonic pachymetry and digital image analyses of the histopathological sections in any of the groups (Fig. 2). The calculated percentage of corneal resection on the photomicrograph in G1 was significantly different ($p = 0.013$) from the desired percentage of resection (Fig. 2).

The stroma of the air-injected cornea above the needle insertion layer was severely deformed by the small air bubbles relative to the normal cornea (panels A and B in Fig. 3). The most deformed stromal fiber due to air bubbles was removed

Table 1. Corneal thickness at each measurement site

	Corneal thickness pre-operation (μm)*					Mean ± SD	*p* value†
	Central	Inferior	Superior	Nasal	Temporal		
G1	984.1 ± 3.1	974.3 ± 17.7	979.0 ± 13.0	969.7 ± 14.2	976.1 ± 16.4	976.6 ± 5.4	0.569
G2	995.7 ± 5.8	987.3 ± 7.7	985.7 ± 9.0	991.5 ± 5.8	988.2 ± 8.3	989.7 ± 4.0	0.264
G3	1021.2 ± 41.8	1011.4 ± 47.3	995.1 ± 14.2	993.4 ± 14.4	993.7 ± 15.5	1003.0 ± 12.7	0.502
G4	972.0 ± 19.9	968.5 ± 27.1	969.7 ± 26.6	967.2 ± 26.4	969.6 ± 23.9	969.4 ± 1.8	0.999
	Corneal thickness post-operation (μm)*					Mean ± SD	*p* value†
	Central	Inferior	Superior	Nasal	Temporal		
G1	616.9 ± 34.2	612.5 ± 31.3	622.0 ± 53.9	616.7 ± 56.9	617.1 ± 55.0	617.0 ± 3.4	0.999
G2	621.5 ± 2.8	613.3 ± 2.2	610.0 ± 5.4	617.9 ± 2.8	613.4 ± 2.2	615.2 ± 4.5	0.749
G3	503.1 ± 51.7	500.5 ± 56.9	504.1 ± 55.3	500.4 ± 64.2	501.2 ± 61.5	501.9 ± 1.6	0.999
G4	250.8 ± 19.2	251.3 ± 27.1	257.8 ± 28.6	253.9 ± 24.6	250.4 ± 25.5	252.8 ± 3.1	0.989
	Resected corneal thickness (μm)*					Mean ± SD	*p* value†
	Central	Inferior	Superior	Nasal	Temporal		
G1	367.3 ± 33.8	361.9 ± 46.5	357 ± 42.3	352.9 ± 53.2	359 ± 42.1	359.6 ± 5.4	0.989
G2	374.2 ± 5.0	374.0 ± 9.3	375.7 ± 13.6	373.6 ± 3.8	374.8 ± 8.9	374.5 ± 0.8	0.996
G3	518.1 ± 57.7	510.9 ± 69.0	491.1 ± 58.4	493 ± 65.2	492.5 ± 53.3	501.1 ± 12.5	0.930
G4	721.2 ± 21.4	717.2 ± 32.7	711.9 ± 35.5	713.3 ± 37.8	719.2 ± 35.2	716.6 ± 3.9	0.990

G1, 250 μm trephined group (n = 10); G2, 375 μm trephined group (n = 10); G3, 500 μm trephined group (n = 10); G4, 750 μm trephined group (n = 10) for resection using air assisted lamellar keratectomy. *The values represent the mean ± standard deviation (SD). †One-way analysis of variance was used to investigate differences between measurement sites in each group followed by a Bonferroni's post-hoc test.

Table 2. Measurement of the mean resected corneal thickness in each group

	Mean corneal thickness (μm)*			Trephined corneal depth (μm)	*p* value†
	Pre	Post	Resected		
G1	976.6 ± 5.4	617.0 ± 3.4	359.6 ± 5.4	250	< 0.001‡
G2	989.7 ± 4.0	615.2 ± 4.5	374.5 ± 0.8	375	0.214
G3	1003.0 ± 12.7	501.9 ± 1.6	501.1 ± 12.5	500	0.381
G4	969.4 ± 1.8	252.8 ± 3.1	716.6 ± 3.9	750	0.439

*Values represent the mean ± SD. †Significant differences within the same groups between the mean ablated corneal thickness and trephined corneal depth for resection were identified by the Student's *t*-test. ‡Statistically significant.

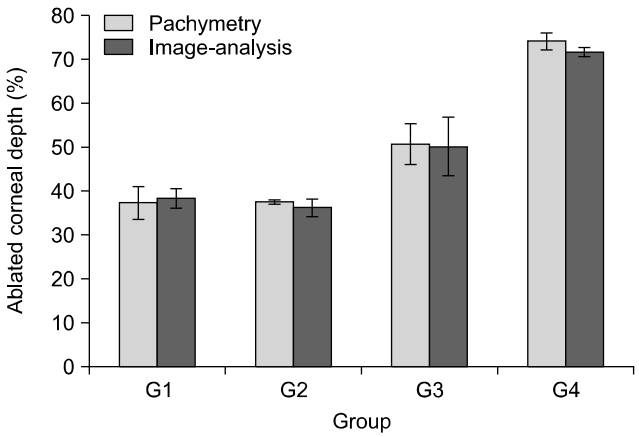

Fig. 2. Ablated corneal thickness (%) calculated based on the pachymetry and photomicrographic image analyses results in each group; G1 = 250 μm, G2 = 375 μm, G3 = 500 μm, G4 = 750 μm trephine for resection.

after resection; hence, the surface of the wounded cornea was smooth following application of air assisted lamellar keratectomy (panel C in Fig. 3C)Several small bubbles inserted into the stroma at the levels of the trephination gutter paralleled the stromal fibril layer on the outside margin of the trephined area.

Corneal haze was noted beginning 7 days after surgery and appeared to peak about 21 days after surgery in both groups (Fig. 4). Clinical corneal haze in the AK group was significantly greater than that in the CK group beginning 14 days after surgery (day 14; $p = 0.036$, day 21; $p = 0.044$, day 28; $p = 0.009$) (Fig. 5A). Furthermore, the quantity of corneal haze was more developed in the AK group than in the CK group from 14 days after surgery ($p < 0.001$) (panel B in Fig. 5).

The corneal sections of the canine eyes showed a distinct stromal remodeling pattern in the AK group relative to the normal cornea and the CK group upon PAS staining (panels A-C in Fig. 6). Alpha-SMA-positive cells were detected

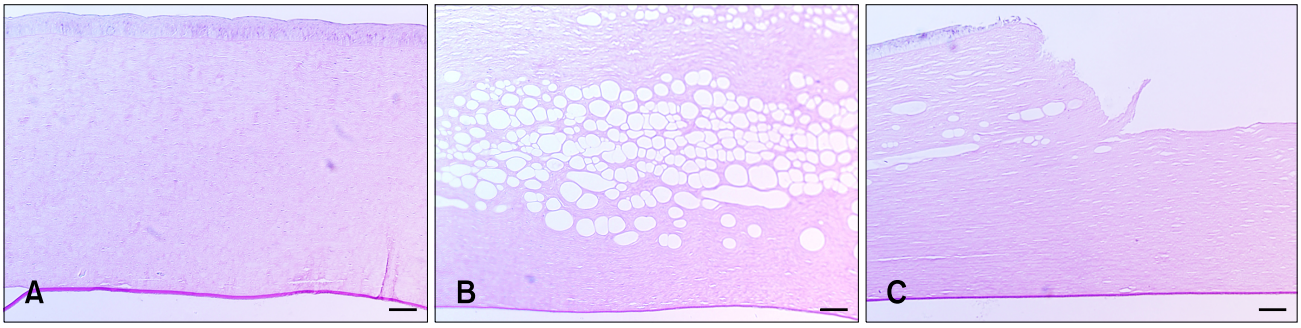

Fig. 3. Photomicrograph of a porcine cornea with periodic acid Schiff (PAS) stain. (A) Normal porcine cornea showing aligned stromal layers. (B) Stroma of the air-injected cornea was deformed by small air bubbles above the layer for needle insertion. (C) After resection by the air assisted lamellar keratectomy showing smooth ablated surface. 200× magnification. Scale bars = 50 μm.

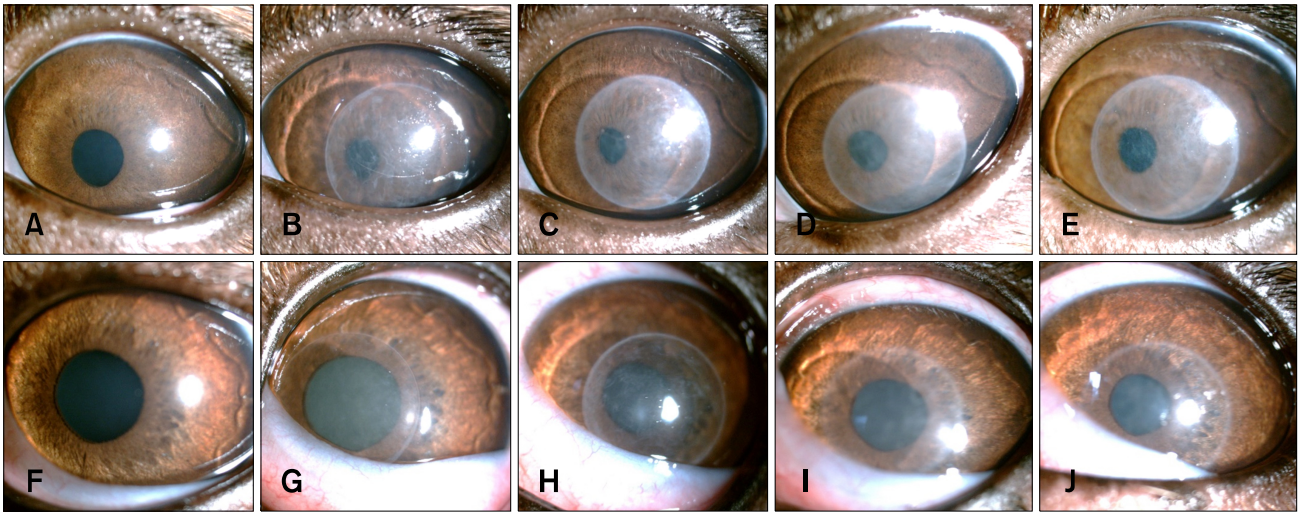

Fig. 4. Slit-lamp biomicroscopy of the corneas with subepithelial haze. Greater corneal haze developed following air assisted lamellar keratectomy (AK group; A–E) than conventional keratectomy (CK group; F–J). The size of the captured corneal section was fixed by controlling the magnification of the slit lamp (10× magnification) under diffuse illumination (45°).

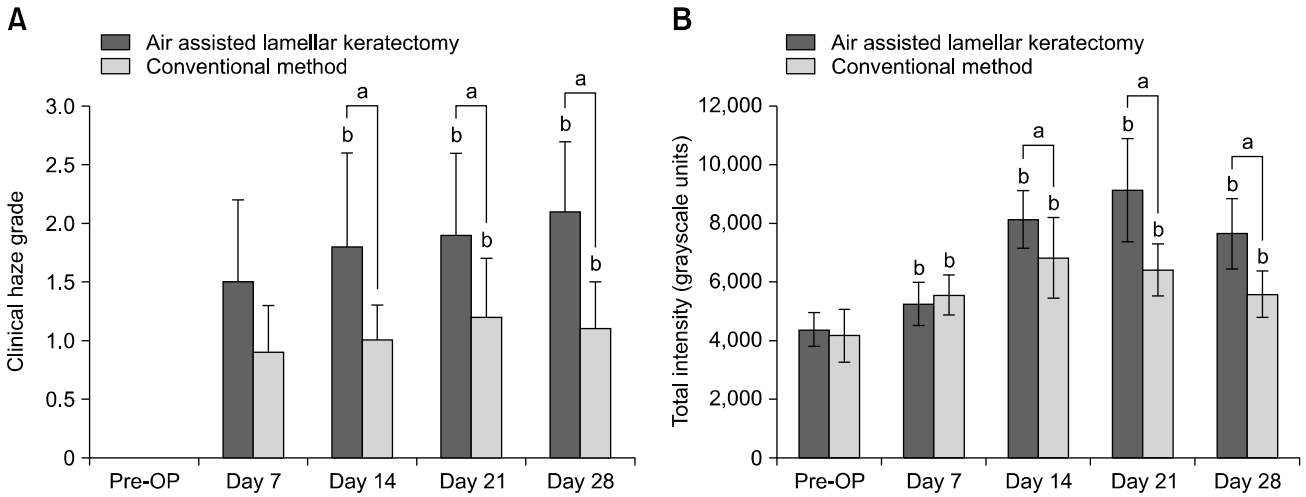

Fig. 5. Corneal haze measurement by quantitative and qualitative methods. (A) Clinical corneal haze grading. (B) Quantification of corneal haze. Significant differences are indicated by Student's *t*-test ($^{a}p < 0.05$) and one-way analysis of variance with Bonferroni's post-hoc test ($^{b}p < 0.05$).

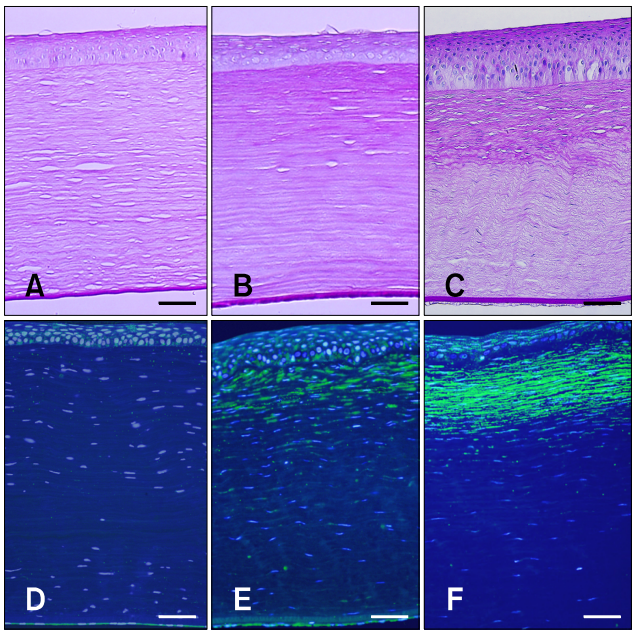

Fig. 6. Histopathological evaluation for the development of corneal haze in the normal cornea (A and D), conventional keratectomy (CK; B and E), and the air assisted lamellar keratectomy (AK; C and E) groups. DAPI-stained nuclei are shown in blue, SMA-stained cells are shown in green. (A–C) PAS stain. 200× magnification. Scale bars = 50 μm. (D–F) Immunohistochemistry stain for α-smooth muscle actin (SMA). 200× magnification. Scale bars = 50 μm.

selectively in the anterior stroma immediately beneath the epithelial basement membrane in the CK and AK groups upon immunohistochemistry (panels D-F in Fig. 6). Total green

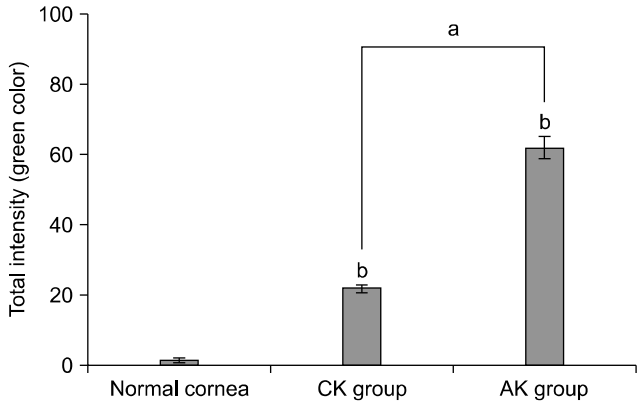

Fig. 7. Total intensity of green color for the quantification of α-SMA positive cells in each group. Significant differences are indicated by Student's *t*-test ($^{a}p < 0.05$) and one-way analysis of variance with Bonferroni's post-hoc test ($^{b}p < 0.05$).

intensity of the entire stroma was significantly enhanced in the CK ($p < 0.001$) and AK groups ($p < 0.001$) relative to that in the normal cornea. Moreover, total green intensity in the AK group was significantly higher than that in the CK group ($p < 0.001$; Fig. 7).

Discussion

Corneal haze is a common complication following corneal surgery that results in diminished corneal transparency [19]. Because the precise mechanisms of the formation of corneal haze are unclear, therapies specifically targeting its prevention are limited. Mitomycin C (MMC) has been widely used to prevent corneal haze following surface ablation for myopia

[22]. However, multiple complications of MMC treatment have been reported, including limbal and scleral necrosis, abnormal wound healing, and loss of keratocytes [18]. These adverse effects have encouraged the development of newer pharmacological agents that can effectively inhibit the formation of corneal haze without causing serious side effects.

Several experimental methods have been used to induce a corneal wound and haze, including mechanical debridement, chemical burns, and superficial keratectomy [17]. Mechanical debridement is primarily used as a model to check the treatment effectiveness of epithelial healing, so the resection is not deep enough to develop sufficient corneal haze. Chemical burning tends to cause loss of keratocytes, further decreasing their density during slow healing injuries [12], and resection depth after applying these methods is difficult to assess owing to loss of transparency. PRK is a superficial keratectomy that employs an excimer laser and has been conducted to achieve accurate ablation [20]. Expensive specialized equipment is needed for this technique, and the haze that develops is grade 1 or less on a scale of four total grades [15], which is insufficient for evaluation of treatment effects. For these reasons, standardized experimental models are needed in this research field.

The first goal of this study was to improve the method of superficial lamellar keratectomy by modifying the big-bubble technique to achieve standardized resection size and depth. We demonstrated that air assisted lamellar keratectomy resulted in uniform resection depth at each of the five measurement sites without expensive laser equipment. Additionally, ablated corneal thickness using this technique was the same as the trephined corneal depth in G2, G3, and G4. The percentage of ablated corneal thickness on the histopathological section calculated with a digital imaging program was not significantly different from the results obtained using ultrasonic pachymetry. In contrast, the resection thickness of G1 was significantly thicker than the desired depth. The trephined depth was not deep enough to insert a needle into in this group and excess air infiltrated under the stroma at the level of needle insertion. For these reasons, more stroma was ablated than desired. Accordingly, the air assisted lamellar keratectomy achieved the standardized resection depth at a trephined corneal depth greater than 375 μm.

The corneal stroma is a precisely formed collagen fibril layer that has a unique parallel arrangement in a mucoid matrix scattered with keratocytes [7]. Because of these stromal structures in the normal cornea, dissection between stromal fibers requires specialized skill. Unlike the normal corneal stroma, the histopathological structure of the air-injected cornea was severely deformed by air bubbles and easily detached using a corneal dissector in this study. Additionally, the injected air bubbles were distributed uniformly over the entire internal area of trephination. These findings indicate that this modified method could be applied more easily and quickly to generate a standardized stromal defect compared to previous models.

Corneal haze developed in all eyes included in this experiment, beginning at day 7 after surgery and appearing to peak about 21 days after surgery. Surface ablation triggers a cascade of physiological events that culminate in mild to severe corneal fibrosis [3]. Modern technologies that involve mechanical removal of the corneal epithelium have demonstrated upregulation of various pro-inflammatory interleukins that indirectly contributes to corneal fibrosis [2]. Haze following PRK may result from corneal wound healing, which is likely to be initiated by keratocyte apoptosis and subsequent over-proliferation of cells [14]. According to our histopathological results, stromal reorganization was observed after healing from the surface resection represented by differentiation of fibroblasts into myofibroblasts with epithelial cell hyperplasia.

Our results show that greater corneal haze developed after applying the air assisted lamellar keratectomy (AK group) than after conventional keratectomy (CK group). Additionally, α-smooth muscle actin (SMA)-positive cells were significantly more numerous in the AK group than those in the CK group upon immunohistochemical evaluation. Expression of α-SMA in fibroblasts is a specific marker of myofibroblast differentiation [10]. The morphological and immunohistochemical findings suggest that more keratocytes were replaced by smooth muscle-like myofibroblasts during wound healing after the air assisted lamellar keratectomy. Mechanical tension is an important underlying factor in the molecular mechanisms of tissue repair and fibrosis. Mechanical stress induces myofibroblast differentiation in human corneal fibroblasts [4,8]. Thus, it seems reasonable to conclude that the air assisted lamellar keratectomy could induce more severe corneal haze due to myofibroblasts after the mechanical tension induced by injecting air bubbles. The stromal structure was severely deformed by the injected air, which is an indication of air bubbles generating mechanical tension on stromal fibers.

In summary, these results suggest that air assisted lamellar keratectomy can be useful to achieve the desired resection depth of the corneal stroma. The air assisted lamellar keratectomy induced more corneal haze than the conventional method of superficial keratectomy. Therefore, this technique would contribute to improving standardization of the corneal haze model.

Acknowledgments

This research was supported by the Basic Science Research Program through the National Research Foundation of Korea (NRF) funded by the Ministry of Education, Science, and Technology (2012007848), and the College of Veterinary Medicine, Research Institute for Veterinary Science of Seoul National University, Korea.

Conflict of Interest

There is no conflicts of interest.

References

1. **Anwar M, Teichmann KD.** Big-bubble technique to bare Descemet's membrane in anterior lamellar keratoplasty. J Cataract Refract Surg 2002, **28**, 398-403.
2. **Chang SW, Chou SF, Chuang JL.** Mechanical corneal epithelium scraping and ethanol treatment up-regulate cytokine gene expression differently in rabbit cornea. J Refract Surg 2008, **24**, 150-159.
3. **de Medeiros FW, Mohan RR, Suto C, Sinhá S, Bonilha VL, Chaurasia SS, Wilson SE.** Haze development after photorefractive keratectomy: mechanical vs ethanol epithelial removal in rabbits. J Refract Surg 2008, **24**, 923-927.
4. **Eckes B, Zweers MC, Zhang ZG, Hallinger R, Mauch C, aumailley M, krieg T.** Mechanical tension and integrin α2β1 regulate fibroblast functions. J Investig Dermatol Symp Proc 2006, **11**, 66-72.
5. **Fantes FE, Hanna KD, Waring GO 3rd, Pouliquen Y, Thompson KP, Savoldelli M.** Wound healing after excimer laser keratomileusis (photorefractive keratectomy) in monkeys. Arch Ophthalmol 1990, **108**, 665-675.
6. **Fini ME.** Keratocyte and fibroblast phenotypes in the repairing cornea. Prog Retin Eye Res 1999, **18**, 529-551.
7. **Freund DE, McCally RL, Farrell RA, Cristol SM, L'Hernault NL, Edelhauser HF.** Ultrastructure in anterior and posterior stroma of perfused human and rabbit corneas. Relation to transparency. Invest Ophthalmol Vis Sci 1995, **36**, 1508-1523.
8. **Garrett Q, Khaw PT, Blalock TD, Scheltz GS, Grotendorst GR, Daniels JT.** Involvement of CTGF in TGF-β1-stimulation of myofibroblast differentiation and collagen matrix contraction in the presence of mechanical stress. Invest Ophthalmol Vis Sci 2004, **45**, 1109-1116.
9. **Hu C, Ding Y, Chen J, Liu D, Zhang Y, Ding M, Wang G.** Basic fibroblast growth factor stimulates epithelial cell growth and epithelial wound healing in canine corneas. Vet Ophthalmol 2009, **12**, 170-175.
10. **Jester JV, Petroll WM, Barry PA, Cavanagh HD.** Expression of α-smooth muscle (α-SM) actin during corneal stromal wound healing. Invest Ophthalmol Vis Sci 1995, **36**, 809-819.
11. **McKee HD, Irion LCD, Carley FM, Jhanji V, Brahma AK.** Dissection plane of the clear margin big-bubble in deep anterior lamellar keratoplasty. Cornea 2013, **32**, e51-52.
12. **Lin N, Yee SB, Mitra S, Chuang AZ, Yee RW.** Prediction of corneal haze using an ablation depth/corneal thickness ratio after laser epithelial keratomileusis. J Refract Surg 2004, **20**, 797-802.
13. **Meeka KM, Fullwood NJ.** Corneal and scleral collagens: a microscopist's perspective. Micron 2001, **32**, 261-272.
14. **Mohan RR, Hutcheon AEK, Choi R, Hong J, Lee J, Mohan RR, Ambrósio R Jr, Zieske JD, Wilson SE.** Apoptosis, necrosis, proliferation and myofibroblast generation in the stroma following LASIK and PRK. Exp Eye Res 2003, **76**, 71-87.
15. **Mohan RR, Stapleton WM, Sinha S, Netto MV, Wilson SE.** A novel method for generating corneal haze in anterior stroma of the mouse eye with the excimer laser. Exp Eye Res 2008, **86**, 235-240.
16. **Møller-Pedersen T.** Keratocyte reflectivity and corneal haze. Exp Eye Res 2004, **78**, 553-560.
17. **Rieck P, Assouline M, Savoldelli M, Hartmann C, Jacob C, Pouliquen Y, Courtois Y.** Recombinant human basic fibroblast growth factor (Rh-bFGF) in three different wound models in rabbits: corneal wound healing effect and pharmacology. Exp Eye Res 1992, **54**, 987-998.
18. **Safianik B, Ben-Zion I, Garzozi HJ.** Serious corneoscleral complications after pterygium excision with mitomycin C. Br J Ophthalmol 2002, **86**, 357-358.
19. **Sakimoto T, Rosenblatt MI, Azar DT.** Laser eye surgery for refractive errors. Lancet 2006, **367**, 1432-1447.
20. **Soong HK, Malta JB, Mian SI, Juhasz T.** Femtosecond laser-assisted lamellar keratopalsty. Arq Bras Oftalmol 2008, **71**, 601-606.
21. **Stepp MA, Zieske JD, Trinkaus-Randall V, Kyne BM, Pal-Ghosh S, Tadvalkar G, Pajoohesh-Ganji A.** Wounding the cornea to learn how it heals. Exp Eye Res 2014, **121**, 178-193.
22. **Teus MA, de Benito-Llopis L, Alió JL.** Mitomycin C in corneal refractive surgery. Surv Ophthalmol 2009, **54**, 487-502.
23. **Yang G, Espandar L, Mamalis N, Prestwich GD.** A cross-linked hyaluronan gel accelerates healing of corneal epithelial abrasion and alkali burn injuries in rabbits. Vet Ophthalmol 2010, **13**, 144-150.